Theoretical and Applied Climatology
https://doi.org/10.1007/s00704-018-2581-7

ORIGINAL PAPER

Recent evolution of glaciers in Western Asia in response to global warming: the case study of Mount Ararat, Turkey

V. Baldasso[1] · A. Soncini[1] · R. S. Azzoni[2] · G. Diolaiuti[2] · C. Smiraglia[3] · D. Bocchiola[1,4]

Received: 23 December 2017 / Accepted: 25 July 2018
© Springer-Verlag GmbH Austria, part of Springer Nature 2018

Abstract
We here investigated the recent (1976–2014) evolution of the Ararat mountain glaciers, paradigmatic of the evolution of ice bodies in Western Asia and the Caucasus. We gathered ice cover maps, including debris cover from different sources, to depict glaciers' extension, and its variation under recent climate patterns. We then gathered data of (daily/monthly) weather variables (temperature, precipitation, snow cover depth) from two local stations managed by Turkish State Meteorological Service, which we subsequently analyzed to assess the presence of significant trends. We used the recently developed, weather-driven glaciological model *Poly-Ice*, able to mimic distributed ice and snow melt, mass budget, and gravity-driven ice flow of glaciers, to reproduce recent evolution of the Ararat ice bodies. We found a measurable decrease of the area (− 2.38 km^2, − 30% of the initial area, − 0.06 km^2 year^{-1}) of the Ararat glaciers, including loss of ice under debris covered tongue (− 1.99 km^2, − 70% of the initial area), driven by significantly increasing temperature especially in spring (+ 0.05 °C year^{-1}). Using our Poly-Ice model, we could (i) mechanistically reproduce the response of the glaciers to the changing climate patterns, (ii) confirm faster downwasting ever since the 1990s under increasing temperature, and (iii) highlight decreased winter snow cover at thaw at the highest altitudes ever since the 1990s, further driving ice melt. Such physically based tool will further allow to project forward the dynamics of these glaciers under future climate. Our results are fully consistent with the present know how of glaciers' retreat from Europe to Caucasus, and Central and Southern Asia, and contribute to the ongoing discussion about retreating glaciers worldwide.

Keywords Ararat glacier · Climate change · Trend assessment · Glacier modeling

1 Introduction

The Ararat mountain (Ağri-Dağı in Turkish, Masis in Armenian, Fig. 1) is an ice-capped volcano (de Silva and Lindsay 2015), and a most important glacierized area in the Near East (Williams and Ferrigno 1991; Sarikaya 2012). It is nested in Eastern Anatolia (Turkey), close to the borders with Iran, Armenia, and Azerbaijan. It is made of two volcanic cones, called the Greater Ararat (Buyuk Ağrı), the highest summit of Turkey with 5137 m a.s.l., and the Little Ararat (Kucuk Ağri), reaching 3896 m a.s.l. (Fig. 1). Ararat is placed within a national park called "Ağrı Dağı Milli Parki." The mountain is traditionally considered to host the Noah's Ark, and it is a national symbol of Armenia. The ice cap is known since middle age (Berlitz 1987), and descriptions of glaciers therein were provided in the 1850s (Abich 1847; Parrot 1859). In the 1950s, Imhof (1956) and Blumenthal (1958) gave a description of the area. However, few geological studies were undertaken (Simkin and Siebert 1994; Notsu et al. 1995; Yilmaz et al. 1998; Karakhanian et al. 2002; Sarikaya 2012). The present availability of satellite images allowed to study the ice caps, and their recent evolution (Çiner 2004; Sarıkaya et al. 2011; Sarikaya 2012; Yavaşli et al. 2015). No glaciers' modeling exercise was proposed therein that we know of. The manuscript aims at (i) assessing recent Ararat glaciers' changes (retreat), and their relation to visible climate change in the area, including warming and decrease of snow feeding at the lowest altitudes, and (ii) mechanistically reproducing the dynamics of the Ararat glaciers and their changes in response to climate

✉ D. Bocchiola
daniele.bocchiola@polimi.it

[1] Department of ICA, Politecnico di Milano, L. da Vinci, 32, Milan, Italy

[2] Department of Environmental Science and Policies, Università di Milano, Celoria 2, Milan, Italy

[3] Department of Earth Sciences, Università di Milano, Mangiagalli 34, Milan, Italy

[4] EVK2CNR Committee of Italy, S. Bernardino 145, Bergamo, Italy

Published online: 02 August 2018

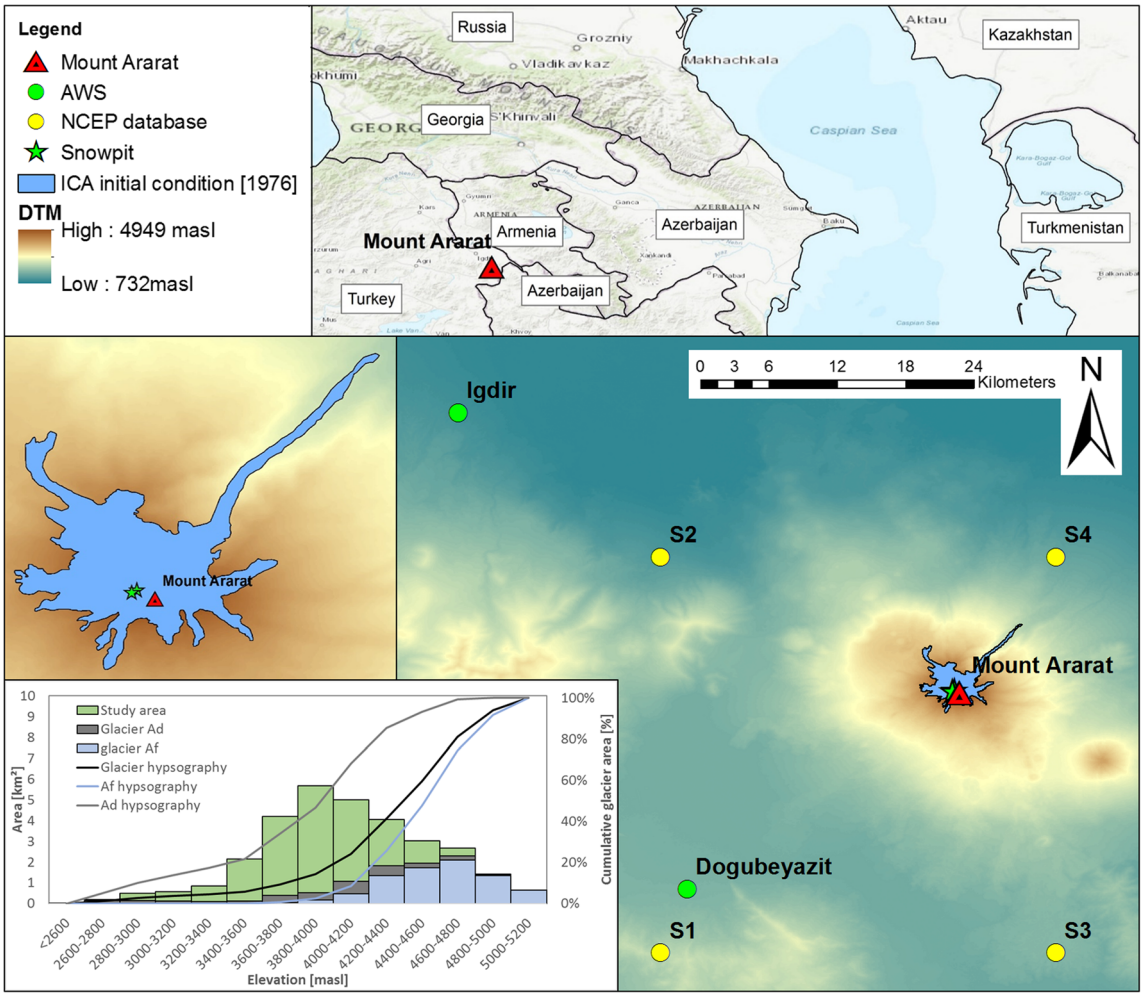


Fig. 1 Mount Ararat. Hypsography and ice cover (2014) reported. A_f is free ice area, and A_d is debris-covered area

patterns. To this purpose, we gathered ice cover maps, including debris cover to provide glaciers' extension and changes therein. We then gathered data of (daily/monthly) weather variables (temperature, precipitation, snow cover depth) from two local automatic weather stations AWSs owned by Turkish State Meteorological Service TSMS, and we analyzed these data to assess the presence of significant trends, possibly affecting glaciers' retreat. We compared the observable weather patterns with the glaciers' cover variations, and we reviewed the potential impact of climate on ice bodies. We then used the recently developed glacio-hydrological model *Poly-Ice* (e.g., Soncini et al. 2016, 2017; Aili et al. 2018; Bocchiola et al. 2018) to mimic the behavior of the Ararat glaciers in response to observed weather patterns, to strengthen the hypothesis of climate driven retreat in the last four decades. Our work here builds partially upon some previous works, aimed at measuring ice cover extent in the area (Sarikaya 2012), and at describing the local morphology, including bare and debris-covered ice (Azzoni et al. 2017). However, our work moves forward because (i) we provide more complete depiction of the glaciers' evolution including debris-free and debris-covered areas; (ii) we pursue a statistically consistent assessment of the trends of key meteorological variables, to be linked to glacier retreat; (iii) we innovatively provide distributed 2D mass budget, and ice flow modeling of this topographically complex ice cap, including the debris-covered area, which we use to substantiate our conjectures about the impact of the recent climate variations on the dynamics of the glaciers; and (iv) we provide a tool for assessing the potential future behavior of the glaciers on the Ararat mountain under future climate change. Moreover, we exploit information from a recent survey during summer 2014. Our results can therefore contribute to the ongoing discussion about retreating glaciers in Europe and Asia, and worldwide.

2 Case study: Mount Ararat

2.1 Geomorphology

An updated depiction of the geomorphology of Mount Ararat is provided, e.g., in Azzoni et al. (2017). In short, Ararat mountain entails about 1150 km^3 of andesitic, basaltic, and

dacitic lavas, and dacitic and pyroclastic rhyolitic debris (Yilmaz et al. 1998). Little Ararat is a steep conical stratovolcano, whereas Great Ararat takes its shape from partial destruction of a series of basaltic andesite, andesite cinder cones, and dacite lava domes (Simkin and Siebert 1994). The two volcanoes resulted from intense magmatic activity in the area of Eastern Anatolia Accretionary Complex (Keskin 2003).

2.2 Climate

The semi-arid climate of this area is influenced by the continental climate of the Anatolian plateau, and it shows a great variability throughout the year. Average annual precipitation (1976–2014) at Dogubeyazit (20 km southwest of the study area, 1592 m a.s.l.) is 408 mm, although actual precipitation amount upon the Ararat mountain is probably higher, due to orographic effects. In Igdir (30 km north of Ararat, 858 m a.s.l.), precipitation yearly (1986–2014) reaches 298 mm. The mean annual air temperature at Dogubeyazit is ca. + 9.2 °C, with summer average of + 27.7 °C and winter low of − 6.1 °C, with Igdir displaying 12.3, + 32.1, and − 3.8 °C, respectively. Recent assessment of long-term (1970–2009) climate trends displayed a general increase of the measured air temperatures, but no visible changes in precipitation (Sarikaya 2012). Such trend detection exercises were based only upon linear regression, and no assessment of snow cover was pursued, so more complex assessment is developed here.

2.3 Glaciology of the area

Few field data on glaciation of the area are available. The first studies were reported by Imhof (1956) and Blumenthal (1958). They observed 11 outlet glaciers emerging from a summit ice cap covering about 10 km^2, in accordance with Hughes (2014). In the 1950s, the glaciers of Ararat reached down to 3900 m a.s.l. and to 4200 m a.s.l. on the north- and south-facing slopes, respectively. More detailed analysis of the glacierized area was proposed by Kurter (1991), using Landsat satellite imagery interpretation. Sarikaya (2012) and Sarikaya and Tekeli (2014), in a remote-sensing-based inventory of Turkish glaciers, analyzed the recession of Ararat ice caps, finding a total surface area of 7.98 ± 0.80 km^2 in 1976, decreasing to 5.66 ± 0.57 km^2 in 2011, similarly estimated by Yavaşli et al. (2015). Concerning local and regional glacial advances in the Pleistocene, few studies were dedicated to Mount Ararat. Çiner (2004), Sarikaya et al. (2011), Sarikaya and Çiner (2014), and Akçar et al. (2015) evidenced wide Pleistocene glaciations upon the Taurus Mountains, on the north slopes of the Eastern Black Sea Mountains, the Mounts Erciyes and Süphan, and Ararat/Ağri Dağı. For the last glacial maximum (LGM), they identified a mean snow line altitude of ca. 2500 m a.s.l., unless for Ararat, where it was located at ca. 3000 m a.s.l. No evidence of glacier extent is available before the LGM, in contrast with other Mediterranean regions (Greece, the Balkans, central and southern Italy, Iberia, and the Atlas). The glacierized area on top of the volcano (Fig. 3 in Azzoni et al. 2017) is classified as an ice cap (Williams and Ferrigno 1991), and four main ice bodies flow downward. One is a debris-free, double-tongued glacier (no local name available), on the Western flank. The three other bodies are the Parrot Glacier, on the Northeast flank, the Cehemmen Glacier nested in the Ahora Gorge on the Northeastern flank, and the Parachute glacier (name given by a local guide), on the Southwest side near the main climbing track (Figs. 4 and 5, in Azzoni et al. 2017). These glaciers display notable debris cover depth D_d (i.e., from our field investigations during summer 2014 $D_d > 20$ cm). Knowingly, debris cover mainly reduces surface melting (Diolaiuti et al. 2009; Bocchiola et al. 2010; Soncini et al. 2015, 2016; Azzoni et al. 2016). Supraglacial debris also prevented accurate mapping of the glacier boundaries hitherto. In the lack of field surveys, mid-resolution information from satellite imagery is not enough to recognize the boundaries of debris-covered areas. Our field surveys in 2014, reported below, allowed for the first time to detect and map debris-covered glaciers' snouts. We found a number of sources to define the debris-free area during 1976–2011 (Sarikaya and Tekeli 2014), and the total area during 1990–2014, which we used to (i) define recent glaciers' retreat and (ii) tune the Poly-Ice model for ice cover dynamic simulation.

2.4 Water-related landforms and hydrology

The hydrographic network of the Ararat mountain displays a radial pattern, according to its conic shape and geometry. The main streams appear at the lowest elevations, whereas ephemeral fluvial traces are at the highest elevations. During our survey, we found that the majority of streams are fed by ice and snow melt, and feature sporadic regime, decreasing at night in lack of melting. Due to the permeability of the bedrock, water mostly infiltrates. No hydrological measurements could be taken to validate water-related conjectures for the area.

3 Data and methods

3.1 Field expedition in July 2014.

During July 18–28, 2014, two of the authors participated into a scientific expedition on Mount Ararat, organized by *Club Alpino Italiano* (CAI) to celebrate its 150 years. The expedition involved 11 persons from 7 institutions (see "Acknowledgments" section below). During the expedition, the team pursued a number of activities (Garzonio 2015), namely (i) snow profiling (two trenches, 5030 and 5032 m

a.s.l.) near the Ararat summit, 5050 m a.s.l.; (ii) gathering of supraglacial debris samples, and soot/dust retrieval on the Parrot glacier; (iii) GPS positioning of glacier outlines in spot sites; and (iv) visual assessment of debris cover. Visibly during the survey, ice at elevations higher than 4200 m a.s.l. was covered by fern and fresh snow. Snow depth *HS* was thin, ranging from 5 to 10 cm near the Ararat summit, and up to 100 cm on the Western Plateau. The pattern of snow coverage is driven by wind, mainly SW-oriented in winter and N-NE oriented in summer (Azzoni et al. 2017).

3.2 Topography and ice cover

Debris-free glaciers' area could be mapped during 1976–2011 (six dates) using the data from Sarikaya (2012) and Sarikaya and Tekeli (2014), based upon images from Landsat and ASTER (Table 1). Also, the total glacier area, including debris cover, was estimated here for 1990, 2010, and 2014. Glacier outlines from different remote-sensing sources were manually digitalized in ArcMap. The 1990 ice surface was obtained from SPOT 1 images (10-m spatial resolution). The 2010 outlines were derived from Google Earth™ (spatial resolution 2 m), and the 2014 outlines were obtained from PLEIADES (spatial resolution 0.5 m). For each year, we also assessed debris-covered area. To estimate the potential error affecting glacier limits, we applied the method by Vögtle and Schilling (1999), also used, e.g., for the Alpine (Diolaiuti et al. 2012a, b; Smiraglia et al. 2015) and Karakoram glaciers (Minora et al. 2015a, 2016). The accuracy for each glacier was evaluated by buffering the perimeters, with an uncertainty area equal to half the resolution of pixels (here, ca. 2 m). Accuracy of glacier coverage was then assessed by the root of the squared sum of buffer areas. Thanks to the high resolution of satellite imagery and accurate manual mapping, glacier area estimates featured an error less than ± 1%. Exceptions occur in the case of debris-covered glaciers (Kirkbride 2011; Smiraglia and Diolaiuti 2011). The presence of supraglacial debris makes glacier mapping more complex and increases the uncertainty in mapping glacier limits, increasing error up to ± 10% (Smiraglia et al. 2015). To reduce such error, we used the glacier outlines acquired by differential GPS surveys during our field work. ASTER Global DEM (2014, 30-m spatial resolution) was used to model topography. The land cover (i.e., the glaciers' covered area) is entirely bare rocks, so no land use map was necessary. For full account of the method for glaciers' cover assessment and geomorphology of the Ararat, refer to Azzoni et al. (2017).

3.3 Climate data analysis

Using the weather data from the Turkish State Meteorological Service (1976–2014) in two most complete

Table 1 Available database

Station/measure	Alt (m. a.s.l.)	Lat (°N)	Lon (°E)	Variable	Resolution used	Period
Dogubeyazit	1592	39.547	44.084	*T*, *R*, *HS*	Daily	1976–2014
Igdir	858	39.923	43.903	*T*, *R*, *HS*	Daily	1976–2014
S1	2143	39.497	44.063	*T*, *P*	Daily	1976–2014
S2	1130	39.809	44.064	*T*, *P*	Daily	1976–2014
S3	1582	39.497	44.375	*T*, *P*	Daily	1976–2014
S4	1333	39.809	44.375	*T*, *P*	Daily	1976–2014
Snow trenches	5032	39.704	44.295	*HS*, ρ_s	1 day	July 24
Debris cover	5030 ca. 3000–4000	39.703 Sparse	44.293 Sparse	D_d	Few days	July 21–26
Satellite data						
Device	Date	Variable	Res. (m)	Source		
Landsat MSS	August 1976	A_f	80	Sarikaya (2012), Sarikaya and Tekeli (2014)		
Landsat TM	October 1984	A_f	30	Sarikaya (2012), Sarikaya and Tekeli (2014)		
Landsat TM	August 1989	A_f	30	Sarikaya (2012), Sarikaya and Tekeli (2014)		
Landsat ETM+	August 2000	A_f	30	Sarikaya (2012), Sarikaya and Tekeli (2014)		
Aster L1A	September 2002	A_f	15	Sarikaya (2012), Sarikaya and Tekeli (2014)		
Aster L1A	September 2011	A_f	15	Sarikaya (2012), Sarikaya and Tekeli (2014)		
Spot 1	August 1990	A_t, A_d	10	Azzoni et al. (2017), this paper		
Google Earth	August 2010	A_t, A_d	2	Azzoni et al. (2017), this paper		
Pleiades	August 2014	A_t, A_d	0.5	Azzoni et al. (2017), this paper		

T temperature, *R* rainfall, *P* precipitation, *HS* snow height, ρ_s snowpack density, A_f debris-free ice-covered area, A_t total ice-covered area, A_d debris-covered area

stations of Igdir and Dogubeyazit, we derived seasonal (JFM, AMJ, JAS, OND) and yearly average values during 1976–2014, including mean temperature T_{mean}, max temperature T_{max}, min temperature T_{min}, snow depth HS, and (total) precipitation P. These data are investigated for trends using linear regression (LR) analysis, the non-parametric Mann-Kendall (MK) test, and moving average approach (e.g., Bocchiola and Diolaiuti 2010, 2013). The significance of LR during the period of observations is given by a p value ($p = 5\%$, e.g.). Multiple trends could be identified in the time series analysis, e.g., by assessing slope changes (see, e.g., Bocchiola 2014). However, in view of the relative shortness of the series, a single slope regression analysis is carried out. Mann-Kendall test is a non-parametric test, independent from hypothesis about the nature of the trend, and widely used to assess significance of trends in time series (Zhang et al. 2000; Bocchiola et al. 2008). Here, MK test was applied to raw data, with no pre-whitening (Yue and Wang 2002). Upon visual inspection, no evident break points or unexpected abrupt changes were found, and given that no modification of the stations' status was flagged, we did not carry out any homogenization procedure. Then, we investigated the correlation of the weather variables against anomalies (vs long-term average) of the Northern Atlantic Oscillation (NAO) index (e.g., Osborn 2004), during 1976–2014. Further on, we tested the hypothesis that the temperature evolution in the region is linked to warming at a global scale. We thus investigated the correlation between global temperature anomaly DTG (Brohan et al. 2006) and temperature at the stations.

3.4 *Poly-Ice* model

To mimic the dynamics of the Ararat glaciers, we used here the Poly-Ice model. Poly-Ice model is part of a larger, hydrological model called *Poly-Hydro*, usable to assess water budget and stream flows in high-altitude catchments. Both such models were developed by the personnel of Polytechnic of Milan Engineering School, and accordingly the name of the model. Poly-Ice takes care of ice mass budget, and flow dynamics, and feeds Poly-Hydro model with outputs of snow on ice melt, and glaciers' ice melt, necessary for water budget of the catchment. The Poly-Ice and Poly-Hydro models were used jointly recently in a number of works (Migliavacca et al. 2015; Soncini et al. 2015, 2016, 2017; Aili et al. 2018; Bocchiola et al. 2018), demonstrating noteworthy flexibility of both for modeling of ice bodies and hydrological budgeting of high-altitude catchments. Here, Poly-Ice model was used in a stand-alone version, because hydrological modeling was not necessary as reported. To complement the data from the TSMS for assessment of the temperature altitudinal lapse rate, we used the reanalysis data from the National Center for Environmental Prediction (NCEP) produced by the Climate Forecast System Reanalysis (CFSR). We could find NCEP data for 3 stations (Fig. 1, Table 1), namely S1 Southwest of Ararat, S3 in Southeast, and S4 in Northeast. For precipitation, we could use 4 stations of NCEP (S1, S3, S4, plus S2, Northwest of Ararat). The temperature lapse rate (until a maximum altitude of 2100 m a.s.l. in S1) varies from −2.8 °C km^{-1} in January, to −6.2 °C km^{-1} in April. The precipitation lapse rate changes from ca. 20 mm km^{-1} (August and September) to ca. 11 mm km^{-1} in May. For modeling purposes, distributed temperature and precipitation (upon a 30 × 30 m^2 grid) was calculated using the so calculated lapse rates. Snow precipitation is simulated whenever local temperature within a given cell is below 0 °C. Fresh snow density is taken as $\rho_n = 120$ kg m^{-3} (Bocchiola and Rosso 2007). Ablation of bare/debris-covered ice and of snow have to be assessed to simulate glaciers' budget. Here, both these processes were modeled by way of a mixed (radiation plus temperature) or enhanced degree-day approach (Soncini et al. 2016), namely

$$\begin{aligned} M_{i,s} &= \left(TMF_{i,d,s}(T-T_{th}) + RMF_{i,d,s}\left(1-\alpha_{i,d,s}\right) G\right) \quad if \;\; T \geq T_{th} \\ M_{i,s} &= 0 \qquad\qquad\qquad\qquad\qquad\qquad\qquad\qquad if \;\; T < \;\; T_{th} \end{aligned} \tag{1}$$

Therein, $M_{i,s}$ (mm day^{-1}) is the melting of either ice or snow within a cell, $TMF_{i,d,s}$ (mm day^{-1} °C^{-1}) and $RMF_{i,d,s}$ (mm day^{-1} W^{-1} m^2) are the temperature and radiation melting factors for either free ice/debris-covered ice/snow, and $\alpha_{i,d,s}$ is the ice-free ice/debris/snow albedo (see Table 3). T_{th} is an air temperature threshold (0 °C here as from data analysis). G (W m^{-2}) is the theoretical clear sky, topographically corrected global radiation. The distributed incoming solar radiation in a complex topography as here can be estimated as a function of time of the year, latitude, elevation, topography, and cloud cover (Allen et al. 2006; Senese et al. 2016). Here, we calculated the hourly exo-atmospheric radiation incoming on a flat surface (taking into account astronomical and geographical factors only). Then, such radiation was corrected considering the slope and aspect evaluated from the DTM for each cell (considering self-shading). We then modified the solar radiation for passage through the Earth's atmosphere, considering the atmospheric absorption (Kumar et al. 1997), obtaining the incoming clear-sky radiation on a generically oriented surface. Then, the shading due to the local topographic relief and sun position has been evaluated. We used the theoretical radiation instead of the observed one (no cloud cover correction), because (i) no radiation data were available for our period of study and (ii) theoretical radiation values can be used for future projections of glaciers' dynamics and hydrological fluxes (Groppelli et al. 2011; Confortola et al. 2013; Soncini et al. 2016; Bocchiola et al. 2018), so calibration of the melt model

is functional to such application. It is important here to avoid inconsistent "static" glacier cover, unfit for medium- to long-term assessment of ice bodies, and especially for projection of hydrological scenarios (e.g., Soncini et al. 2015, 2016, 2017). Poly-Ice mimics ice flow as driven by gravity (Oerlemans 2001). We used a simplified force balance and pictured velocity as proportional to shear stress raised to n, i.e., the exponent of Glen's flow law ($n = 3$, Wallinga and van de Wal 1998; Cuffey and Paterson 2010). When basal shear stress τ_b (Pa) is either known or estimated, and accounting for both deformation and sliding velocity as governed by τ_b, it is possible to model depth averaged ice velocity as

$$V_{ice,\ i} = K_d \tau_{b,i}^n h_{ice,i} + K_s \frac{\tau_{b,i}^n}{h_{ice,i}} \quad (2)$$

with $h_{ice,i}$ (m) ice thickness in the cell i and K_s (m^{-3} $year^{-1}$) and K_d (m^{-1} $year^{-1}$) parameters of basal sliding and internal deformation. Basal shear τ_b in a cell i can be taken as

$$\tau_{b,i} = \rho_i g h_{ice,i} \sin\alpha_i \quad (3)$$

with ρ_i ice density (kg m^{-3}), g gravity acceleration (9.81 ms^{-2}), and α_i local slope. To estimate ice thickness on the whole glacier's surface, we used Eq. 3. We back estimated ice depth $h_{ice,i}$ from values of τ_b given by Baumann and Winkler (2010) as a function of glaciers' extent in altitude (maximum $\tau_b = 150$ kPa). We adopted the 2014 DEM, and initial ice cover as given in 1976 (debris free), and 1990 (debris cover), the oldest available. The Poly-Ice model is here routed on cells with 30×30 m^2 resolution. Model tuning was pursued by iteratively changing some tuning parameters for snow and ice melting in Eq. 1. Snow melt factors TMF_s, and RMF_s were tuned using temperature T_{mean}, and snow depth HS data in the two TSMS stations. We then finely tuned the values so as to obtain snow depth on the glaciers consistent with observations from snow profiling during our field campaign in summer 2014. From observations during the field campaign as reported (see also Azzoni et al. 2017), we hypothesized a debris cover depth $D_d > 20$ cm, that could be assumed to slow down ice melting with respect to free ice conditions (Bocchiola et al. 2010, 2015; Soncini et al. 2015, 2016). Avalanche nourishment on the glaciers is accounted for, by considering terrain slope (Soncini et al. 2015). When ground slope is larger than a given threshold, progressively more snow detaches (linearly increasing from 0 to 1 within a slop of 30°–60°), and falls in the nearest cell downstream, where it could melt or start transformation into ice. Once a year, 10% of snow surviving at the end of the ablation season becomes new ice (i.e., full ice formation requires 10 years, Soncini et al. 2016, 2017). The flow parameters in Eq. 2, K_d and K_s, were taken as in recent literature (Soncini et al. 2015, 2016, 2017), and slightly tuned to fit area changes as from our satellite images.

4 Results

4.1 Observable glaciers' retreat and climate evolution during 1976–2014

Glaciers' surface (debris-free area A_f) as reported by Sarikaya and Tekeli (2014) changed from 7.87 km^2 in 1976 to 5.68 km^2 in 2011 (− 28% and − 0.06 km^2 $year^{-1}$). Total area (A_t, including debris cover) estimated here changed from 10.70 km^2 in 1990 to 6.33 km^2 in 2014 (− 41%, − 0.17 km^2 $year^{-1}$). Accordingly, rapid retreat occurred in the last 40 years or so. In Fig. 2, we report maps of A_f and A_t during 1976–2014. In Table 2, we report a resume of the trends' assessment exercise. Total precipitation P_{tot} and rainfall R remained constant during the study period, unless for a slight increase of both in Igdir during spring AMJ (+ 0.65 mm $year^{-1}$ of both). In Fig. 3, we report T_{mean} during spring AMJ, and yearly Y in Dogubeyazit, the closest station we have to Ararat mountain, together with the area of glaciers A_f and A_t. These weather variables are the ones changing most significantly. Also, T_{mean} is used to drive Poly-Ice model. In Fig. 3, we also report the area changes yearly (ΔA_t, ΔA_f, expressed in 10^5 m^2, with positive values indicating a loss of area), as modeled by Poly-Ice. Clearly from Fig. 3, the area changes (all positive, i.e., with mass loss), relatively small until the end of the 1980s, display since 1990 or so increasing values, so being clearly consistent with accelerated glaciers' downwasting as seen from observations (Fig. 2). Also from Fig. 3, for years with particularly high value of T_{mean} during AMJ, the largest ice losses happen (e.g., year 2001, with $T_{mean,AMJ} = 11.5$ °C, and a loss $\Delta A_t = 0.27$ km^2, $\Delta A_f = 0.21$ km^2), with vice versa smallest losses during the mildest years (e.g., year 2007, with $T_{mean,AMJ} = 8.7$ °C, and a loss $\Delta A_t = 0.17$ km^2, $\Delta A_f = 0.12$ km^2), and the ice loss is in good phase with temperature in spring. We therefore argue that significantly increasing spring temperature as reported here during our study period contributed largely to increased downwasting of ice bodies in the area. Such findings seem consistent with several studies worldwide (e.g., in the Alps, Bocchiola and Diolaiuti 2010; Diolaiuti et al. 2012a, b; in the Andes, Minora et al. 2015b; in the Karakoram, Bocchiola and Diolaiuti 2013; Minora et al. 2015a, 2016), where increases of temperature and decreased snow cover in the critical period of spring led to accelerated glacier retreat.

4.2 Poly-Ice model

Model tuning was pursued manually. We pursued repeated simulations with different values of the tuning parameters, reported in Table 3, until the model would provide proper mimicking of the glaciers' area evolution during the control period (1976–2014). In Table 3, we also report the

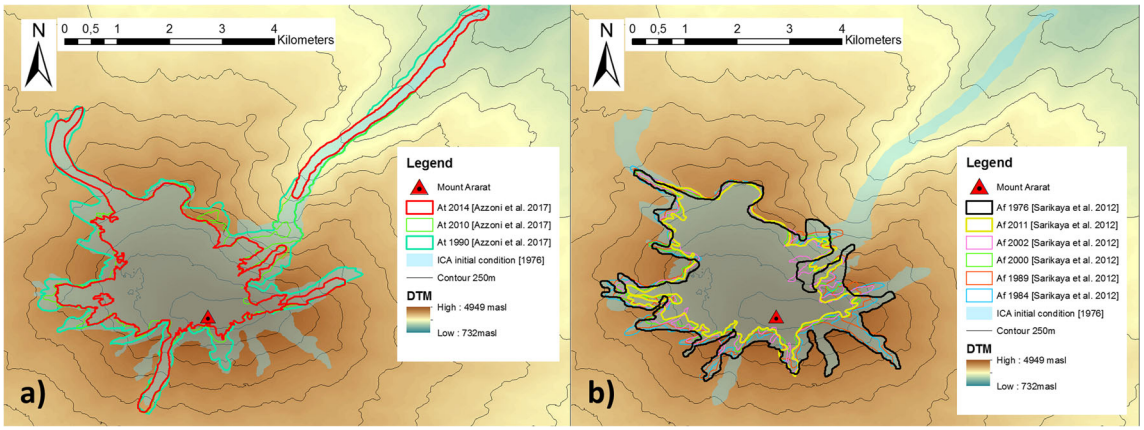


Fig. 2 Ararat glaciers. Ice-covered areas ICA during 1976–2014. **a** Total area A_t. **b** Debris-free area A_f (Sarikaia et al. 2014)

performance of the snow melt module, as given in Eq. 1 by the two parameters $TMF_s = 1.6$ mm day^{-1} °C^{-1} and $RMF_s = 1.2 \times 10^{-3}$ mm day^{-1} W^{-1} m^2. The values so obtained, besides providing an acceptable depiction of snowpack dynamics, are in line with the presently available results in the literature (see Table 2 in Soncini et al. 2017; Table 3 in Aili et al. 2018), and can be used confidently for the assessment of snowpack dynamics. Using these mean snow melt parameters, we obtained a mean $Bias = 2.8\%$, for Igdir and Dogubeyazit, and $R^2 = 0.78$. We also compared simulated snow cover (snow water equivalent (SWE)) on the Ararat summit with observations from two trenches as reported. In spite of being very close to each other, the two trenches provided quite different results, namely with a snow depth of 28 and 100 cm, and a SWE of 122 mm (snowpack density $\rho_s = 437$ kg m^{-3}) and 539 mm ($\rho_s = 539$ kg m^{-3}), respectively. On average, the summit (altitude belt 4900–5100) during summer 2014 (July 23) Poly-Ice model provides on average SWE = 1450 mm, acceptable given the large variability of snow in space as largely acknowledged in the present literature (Bocchiola et al. 2010; Bocchiola and Groppelli 2010; Bocchiola 2010). In Fig. 4, we report modeled ice depth h_{ice} in 1976, used as an initial condition for the Poly-Ice model. A greatest value of 107 m is seen on the Western plateau, with a least thickness on East and South tongue, consistent with previous studies identifying largest thinning in these two areas given exposition and slope (Sarikaya and Tekeli 2014). The model runs at a 30 × 30 m^2 resolution as reported; however to summarize glaciers' evolution, Poly-Ice calculates a number of variables distributed along altitude belts, namely mean glaciers' thickness, mean thickness variation yearly, ice-covered area, ice volume and volume loss yearly, and mean flow velocity. The altitudinal range of simulation (2100–5125 m a.s.l.) was divided into 15 belts, with 200-m vertical jumps. The tuning ice melt parameters are reported in Table 3, namely $TMF_i = 1.2$ mm day^{-1} °C^{-1} and $RMF_i = 2.9 \times 10^{-3}$ mm day^{-1} W^{-1} m^2, in line with recent studies in other areas worldwide (see Minora et al. 2015a; Table 2 in Soncini et al. 2017; Table 3 in Aili et al. 2018). Buried ice melting is here modeled based only on radiation (i.e., with $TMF_i = 0$ in Table 3), consistently with other studies (e.g., Soncini et al. 2016). The radiation melt factor here $RMF_i = 1.8 \times 10^{-3}$ mm day^{-1} W^{-1} m^2 is reasonable, and indicates as expected a decreased effect of solar radiation in the presence of supraglacial debris. Figure 4b provides estimated ice melt depth during 1986–2014 as simulated by the model. Visibly, values as high as 65 m of ice water equivalent melt IWE$_m$ are found. On average on the glacier, Poly-Ice estimated a loss of ca. 40 m IWE.

Ice flow tuning parameters are reported in Table 3, namely $K_s = 2 \times 10^{-21}$ m^{-3} year^{-1} and $K_d = 5 \times 10^{-25}$ m^{-3} year^{-1}, fully consistent with other recent results (see Table 3 in Soncini et al. 2016; Table 2 in Soncini et al. 2017; Table 3 in Aili et al. 2018). The ice-covered area estimates obtained with the Poly-Ice model within each altitude belt are benchmarked against their observed counterparts in the available years.

In Fig. 5, we report the total area A_t and debris-free area A_f simulated by Poly-Ice vs their observed counterparts, together with the simulated debris-covered area A_d. A_d is simulated by the model as substantially constant until 1995 or so, and then decrease in response to ice melting (with a large decrease nearby 2014, as seen in Fig. 2a, with separation of the Northeast debris-covered tongue). In Fig. 6, we report the same areas, distributed as per altitude belts. Visibly, the model mimics reasonably well the total areas A_t (Fig. 5, red dots), even approximating the observed (linear) trend. However as reported, A_t could be estimated for 3 years only. In Fig. 6a, one appreciates the reasonably good capability of the model in assessing A_t as a function of altitude. During 2014, Poly-Ice displays some overestimation for the lowest altitude belts (3500–4500 m a.s.l.). Debris-free area A_f, available for 6 years, seems also reasonably well caught by the model (Fig. 5, blue dots) globally, albeit with some overestimation in the central phase (1985–2000). Also in Fig. 6b, the model depicts well A_f vs altitude, with some overestimation in 2000 at the high altitudes (4500–4900 m a.s.l.).

Table 2 Results of trend assessment tests

Var	Test	Dog Y	Dog JFM	Dog AMJ	Dog JAS	Dog OND	Igdir Y	Igdir JFM	Igdir AMJ	Igdir JAS	Igdir OND
P_{tot} (mm)	LR	− 0.80	0.01	0.58	− 0.92	− 1.12	− 0.59	0.89	0.65	− 0.14	0.80
	LR-p	0.25	0.98	0.25	0.25	0.46	0.13	0.13	*0.02*	0.72	0.40
	MK-p	0.27	0.97	0.24	0.19	0.73	0.16	0.16	*0.02*	0.73	0.35
	MA	0	0	0	0	0	0	0	0	0	0
	NAO	–	–	–	–	–	–	–	–	–	–
	DT_G	–	–	–	–	–	–	–	–	–	–
R (mm)	LR	0.14	0.08	0.58	− 0.05	0.75	− 0.16	0.89	0.65	− 0.17	1.20
	LR-p	0.70	0.89	0.25	0.94	0.59	0.53	0.13	*0.02*	0.61	0.16
	MK-p	0.67	0.80	0.24	0.71	0.45	0.73	0.16	*0.02*	0.69	0.18
	MA	0	0	0	0	0	0	0	0	0	1
	NAO	–	–	–	–	–	–	–	–	–	–
	DT_G	–	–	–	–	–	–	–	–	–	–
T_{mean} (°C)	LR	0.05	0.05	0.02	0.02	0.04	0.05	0.05	0.06	0.03	0.05
	LR-p	0.12	*0.00*	0.14	0.40	*0.02*	0.11	*0.00*	*0.00*	0.08	*0.00*
	MK-p	0.20	*0.00*	*0.04*	0.39	*0.01*	0.14	*0.00*	*0.00*	0.12	*0.00*
	MA	0	0	0	0	*1*	0	0	*1*	0	*1*
	NAO	–	–	–	*− 0.36*	–	–	–	–	*− 0.34*	–
	DT_G	*0.43*	–	*0.40*	–	–	*0.54*	–	*0.42*	*0.57*	–
T_{min} (°C)	LR	0.04	0.03	0.02	0.03	0.03	0.06	0.08	0.10	0.05	0.07
	LR-p	0.18	*0.02*	0.06	0.23	*0.02*	*0.04*	*0.00*	*0.00*	*0.01*	*0.00*
	MK-p	0.27	*0.03*	0.05	0.45	*0.02*	0.12	*0.00*	*0.00*	*0.03*	*0.00*
	MA	0	0	0	0	0	0	*1*	*1*	0	*1*
	NAO	–	–	–	–	–	*− 0.36*	–		*− 0.35*	
	DT_G	*0.38*	–	*0.36*	–	–	*0.70*	–	*0.69*	*0.79*	*0.41*
T_{max} (°C)	LR	0.06	0.06	0.02	0.03	0.04	0.03	0.02	− 0.01	0.01	0.01
	LR-p	0.06	*0.01*	0.27	0.19	*0.01*	0.36	0.26	0.62	0.82	0.39
	MK-p	0.14	*0.02*	0.23	0.16	*0.01*	0.28	0.18	0.59	0.97	0.20
	MA	*1*	0	*1*	0	*1*	0	0	0	0	0
	NAO	–	–	–	–	–	–	–	–	–	–
	DT_G	*0.46*	–	–	–	*0.34*	–	–	–	–	–
HS (cm)	LR	0.45	− 0.07	0.00	− 0.07	0.30	− 0.43	0.00	0.00	0.03	− 0.40
	LR-p	0.28	0.25	–	0.84	0.62	*0.05*	–	–	0.86	0.18
	MK-p	0.65	*0.00*	*0.00*	0.26	0.99	*0.01*	*0.00*	*0.00*	0.25	0.15
	MA	0	0	0	0	0	*1*	0	0	0	*1*
	NAO	–	–	*− 0.36*	–	–	–	–	–	–	–
	DT_G	–	–	–	–	–	–	–	–	–	–

LR is linear regression coefficient (unity^{-1}). LR-p is p val of linear regression. MK is p val of Mann-Kendall test. MA is result of moving average test for stationarity (p val = 5%, 0 means passed, 1 means not pass). NAO/DT_G is correlation coefficient with NAO/DT_G (only in same season), reported when significant (p val = 5%)

Italic means significant values (at 5%)

5 Discussion

5.1 Observed glaciological trends from Western Europe to Southern Asia

The meteorological and glaciological trends of the Ararat region here are consistent with the trends observed recently in Asia (Bocchiola and Diolaiuti 2013; Salerno et al. 2014; Soncini et al. 2015, 2016) and worldwide (e.g., in the Alps, Bocchiola and Diolaiuti 2010; Diolaiuti et al. 2012a, b, and in the Andes, Minora et al. 2015b). The increasing temperatures in the three last decades, and especially during the critical spring season in the presence of substantially unchanged precipitation patterns, have impacted ice cover.

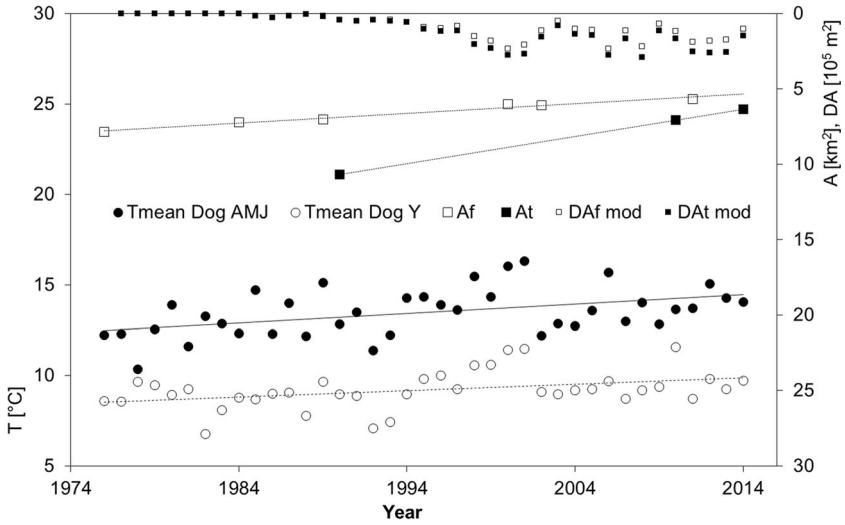


Fig. 3 Ararat. T_{mean} during spring AMJ, and yearly Y in Dogubeyazit, area of glaciers A_f, and A_t, and area changes from the *Poli-Hydro* model ΔA_t, ΔA_f

Albeit no direct measurements of snow cover at the highest altitudes were available here (but at lower altitudes in Dogubayezit at 1592 m a.s.l., where no significant change was observed), one can imagine that decreased snow cover at the highest altitudes during thaw seasons may affect ice melt dynamics, i.e., providing earlier onset of ice melting. In Fig. 7, we report simulated SWE within different altitude belts on the Ararat mountain at spring (i.e., on April 1, conventionally taken as the end of accumulation season, e.g., Bocchiola 2010) averaged for four decades, during 1976–2014. Clearly, in response to increasing temperature during the last four decades, snow cover decreased at the intermediate altitudes, so leaving ice exposed earlier during the melt season. Such effect is largely consistent with observations in the mountains from Europe to Central and Southern Asia.

Among others, Stokes et al. (2006) studied the recent terminus position of glaciers (1600 km^2) in the Caucasus mountains northern of Ararat here using satellite imagery (Landsat TM, and ETM+). They estimated that 94% of the glaciers retreated. Mean retreat rate was estimated into ca. − 8 my^{-1}, with a maximum of − 38 my^{-1}. The largest (> 10 km^2) glaciers retreated twice as fast (− 12 my^{-1}) as the smallest (< 1 km^2, − 6 my^{-1}). The surface area of bare ice reduced by − 10% during 1985–2000. Decrease in their area was primarily driven by increasing temperatures since the 1970s, and especially since the mid-1990s, like seen here (Fig. 3). Stokes et al. (2007) similarly studied changes in supraglacial debris cover and

Table 3 *Poly-Ice* model parameters and goodness-of-fit statistics

Parameter	Unit	Description	Value	Method
$\alpha_{ci,s}$	–	Albedo, ice/debris/snow	0.4/0.2/0.7	Literature
$TMF_{i,d,s}$	mm day^{-1} °C^{-1}	Mean thermal melt factor, ice/debris/snow	*1.2/0/1.6*	A_f, A_t, nivometer
$RMF_{i,d,s}$	mm day^{-1} W^{-1} m^2] × 10^{-3}	Mean radiation melt factor, ice/debris/snow	*2.9/1.8/1.2*	A_f, A_t, nivometer
Dog, $TMF_{ci,s}$	mm day^{-1} °C^{-1}	Dogubayezit thermal factor, snow	*1.89*	A_f, A_t, nivometer
Dog, $RMF_{ci,s}$	[mm day^{-1} W^{-1} m^2] × 10^{-3}	Dogubayezit radiation factor, snow	*1.40*	A_f, A_t, nivometer
Igd, $TMF_{ci,s}$	mm day^{-1} °C^{-1}	Igdir thermal f., snow	*1.30*	A_f, A_t, nivometer
Igd, $RMF_{ci,s}$	[mm day^{-1} W^{-1} m^2] × 10^{-3}	Igdir radiation f., snow	*1.00*	A_f, A_t, nivometer
K_s	m^{-3} year^{-1}	Ice flow basal sliding coeff.	*2.0E*$^{-21}$	Literature, A_f, A_t
K_d	m^{-1} year^{-1}	Ice flow internal deformation coeff.	*5.0E*$^{-25}$	Literature, A_f, A_t
Goodness of fit snow melt				
Station	NSE (site)	Bias (site)	NSE (mean)	Bias (mean)
Igdir	0.79	3.0%	0.78	15.7%
Dogubayezit	0.81	2.9%	0.78	− 10.0%
Aver. (*Dog*, *Igd*)	–	–	0.78	2.8%

Italic values indicate tuning parameters that were calibrated against estimated snow melting at the available nivometers and against and glaciers' area. Snow melt factors and goodness of fit are given for point site and average values

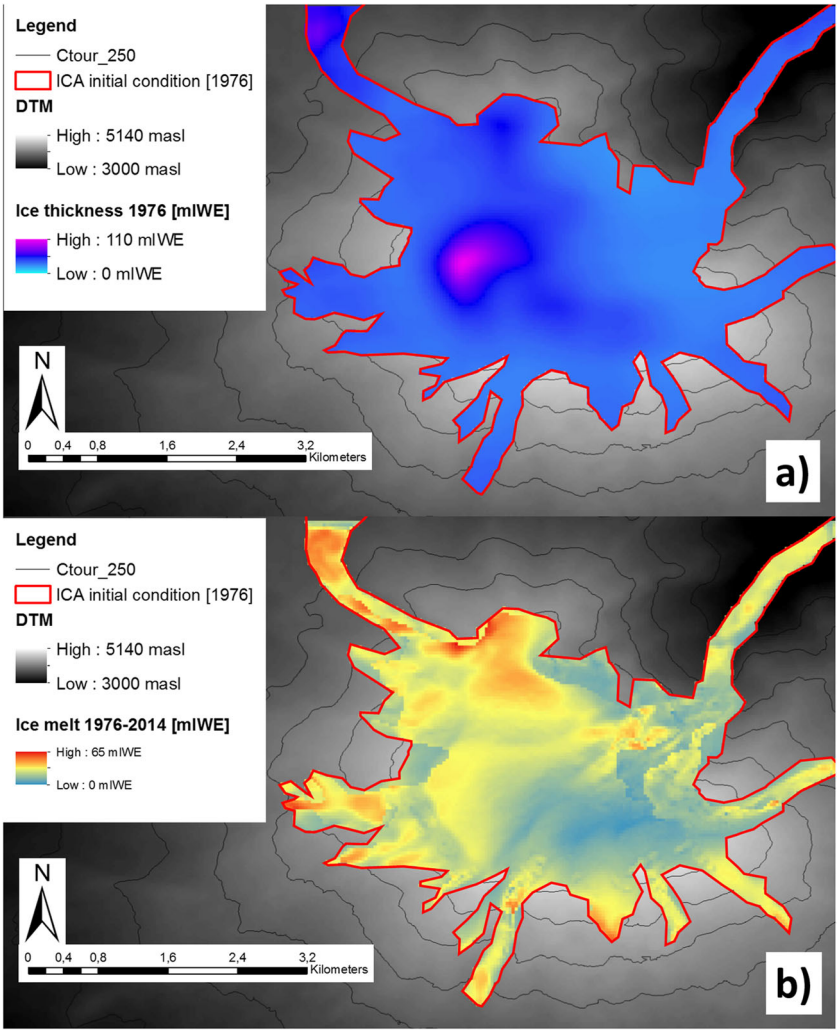


Fig. 4 Ararat glaciers. Ice cover thickness h_{ice}, and ice melt IWE. **a** Ice depth estimated in 1976. **b** Ice melt IWE_m simulated during 1976–2014

supra-/pro-glacial lakes on six glaciers in the Adylsu valley. Supraglacial debris cover ranges from 5 to 25% ca. on individual glaciers, and glacier retreat during 1985–2000 resulted into a + 3 to + 6% increase of debris cover.

Here, we consistently found visible area decrease (− 2.38 km^2, − 30%, − 0.06 km^2 $year^{-1}$), driven by increasing temperature, and decreased snow accumulation. Debris-covered area in our observations decreased ever since the

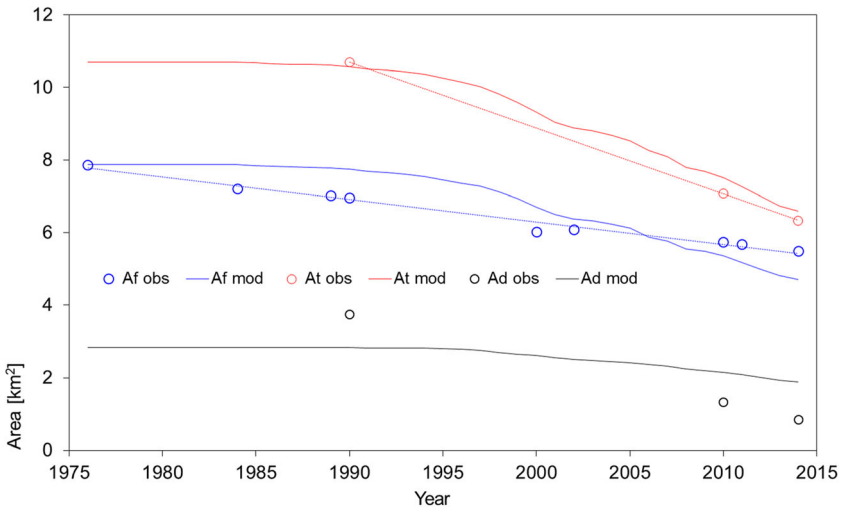


Fig. 5 Ararat glaciers. Total area A_t, and debris-free area A_f as simulated by *Poly-Ice* model vs their observed counterparts. A_d is debris covered as simulated by the model, and from our classification

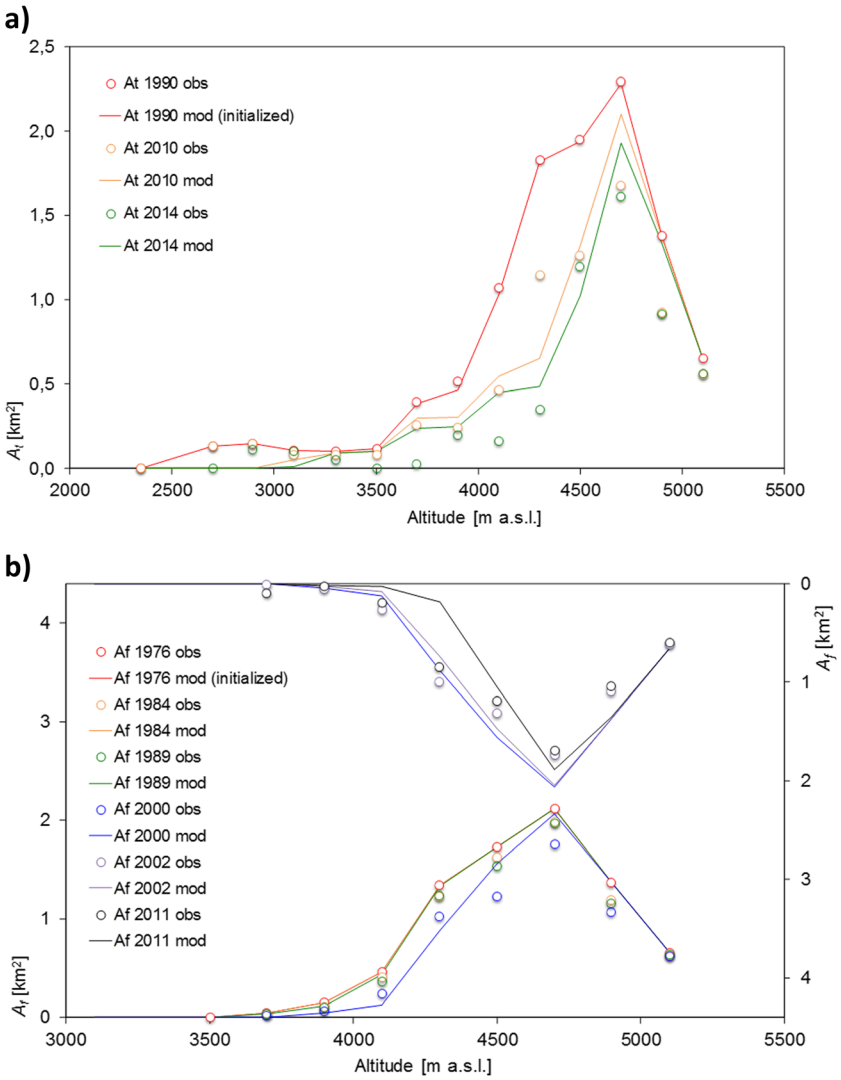


Fig. 6 Ararat glaciers. Total area A_t, and debris-free area A_f distributed as per altitude belts. **a** A_t. **b** A_f

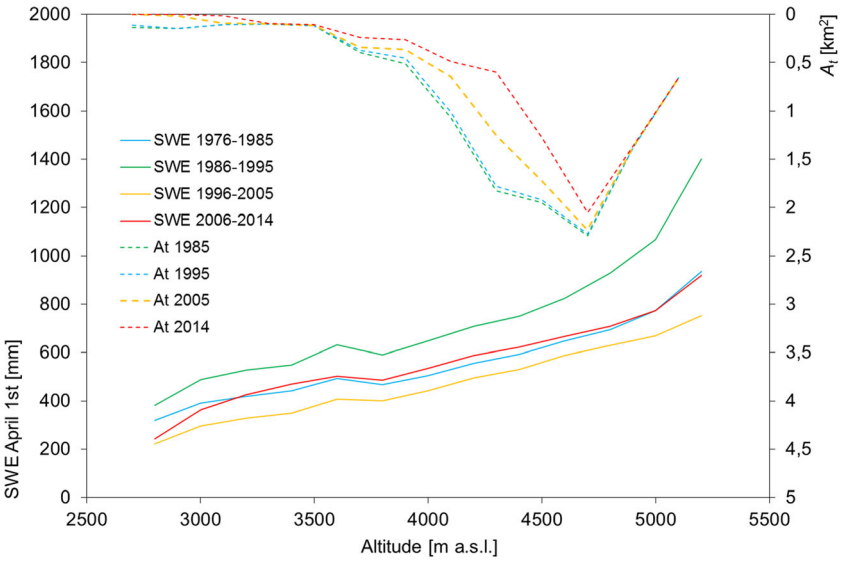


Fig. 7 Ararat. Simulated SWE at April 1 in different altitude belts, averaged for decades during 1976–2014, and total ice-covered area A_t at the end of each decade

1990s (Figs. 2 and 3), mainly by ice melting underneath the debris as simulated by Poly-Ice model. However, the high slope of the Ararat flanks and the cone-like shape geometry seemingly suggest no potential for debris cover increase besides the present covered area at the lowest altitudes.

Narama et al. (2010) investigated recent glacier dynamics in the Tien Shan Mountains of Central Asia (Pskem, Ili-Kungöy, At-Bashy, and SE-Fergana) during 1968–2008. During 1970–2000, glacier area decreased by − 19 to − 9% in different regions. During 2000–2007, only a further decrease of − 5 to 0% occurred, triggered by the ever-rising summer temperatures.

In the Northern Karakoram, recent studies connected signals of slightly increased snow precipitation to substantial stability of the glaciers. Bocchiola and Diolaiuti (2013) and Minora et al. (2016) found slightly increased number of wet days in Gilgit, in the Karakoram range, during 1980–2009, and evidence of constant or even slightly increased ice cover (the "Karakoram Anomaly") in the Central Karakoram National Park (CKNP). Ice-covered area (ICA) therein was 4605.9 km^2 in 2001 and 4606.3 km^2 in 2010, with abundant supraglacial debris cover. Further evidence of slightly increased snow cover area in fall above 1900 m a.s.l. during 2001–2011 seemingly confirms the positive feedback of snow cover. Bocchiola et al. (2011), Minora et al. (2015a), and Soncini et al. (2015) studied recent ice melting on Karakoram glaciers and demonstrated however that under future climate change as projected by the IPCC at 2100, largely decreased snow cover may result in larger glaciers downwasting, so eventually breaking down the Karakoram Anomaly as we know it nowadays.

In the Himalayas (Everest region), Salerno et al. (2014) examined glacier changes on the south side of Mt. Everest during 1962–2011 using optical satellite imagery. They found an area loss of 13.0 km^2 (out of 400 km^2 ca.), with an upward shift of 182 m of the snowline altitude at thaw. Albeit no long-term data of snow depth are available in that area, one may assume that decreased snow availability has impacted glacier recession in the area.

When one considers the Alps of Europe, several studies connected the increased temperature, the decreased amount of snow, and lower number of snowfall events, with glacier downwasting. In Switzerland, Ohlendorf et al. (1997) compared glacier *varves* from glacial Lake Silvaplana against a 127-year climate data series (summer rainfall and temperature, yearly snowfalls NS) from AND AWS station in Sils Maria SMA to assess effects of climate change on Morteratsch and Roseg Glaciers. For 1966–1990, they showed a decrease of number of snowfalls *NS* of about − 0.64 ddy^{-1}. They also found inverse correlation between *NS* and ice melt at thaw, which they explained via decreased albedo from new snow. Seiz and Foppa (2007) reported − 0.22 cm year^{-1} of cumulated snowfall HN_{cum} (linked to *HS*) for SMA during 1864–2006, whereas Wüthrich et al. (2008) reported that the 1864–2005 trend of days with snow pack (D_0) reveals significant decrease in the Swiss Alps, including SMA, implying the effect of snowpack of ice protection.

In the Southern Alps, Bocchiola and Diolaiuti (2010) investigated snowfall days *NS* (1965–2007) from a manual daily station in the Adamello glacier area (24 km^2) in the Italian Alps, finding a widespread decreasing trend of about − 0.6 ddyear^{-1}, which for 42 years leads to 24 too few snowfall days on average. They investigated also snow cover duration for different thresholds. Diolaiuti et al. (2012a) studied snow cover depth at thaw in six glacier groups (92.4 km^2 in 2003) in the central Italian Alps, and found large decrease of snow cover, to which they attribute (together with increasing winter and spring temperature) large glacier variation (117.4 km^2 in 1991, 104.7 km^2 in 1999, and 92.4 km^2 in 2003). Diolaiuti et al. (2012a) investigated Val D'Aosta glaciers in the Western Italian Alps (1975–2005), and found a loss of − 44.3 km^2 (i.e., − 2.8 km^2 year^{-1}), or − 27% of the initial area. They provide evidence of increasing temperature especially during late spring and summer, marked reduction of snowfall and snow cover, to which they largely attribute glacier downwasting.

Eventually, our findings here consistently depict intense downwasting of the ice bodies recently in our target region, as driven by increasing temperature, substantially stable precipitation, and decreased snow availability at the highest altitudes. Such picture is nowadays common to glaciers from the European Alps to Western and Central-Southern Asia (with the exception of the Karakoram anomaly, however possibly temporary as reported), and our results substantiate such conjecture also in the Ararat area.

5.2 Ice flow modeling

Poly-Ice works acceptably well in describing ice depletion during the reference period, so one can assume confidently enough from Fig. 2 that T_{mean} in AMJ is critical for ice melting. Differences between the ice cover simulated by Poly-Ice and the observations may derive from a number of causes. Ice flow as depicted in Eqs. 2 and 3 and the adopted parameters are not tuned directly from flow velocity observations locally (as in, e.g., Soncini et al. 2015, 2016, 2017), but based upon observation of ice-covered areas. Snow/ice melt in Eq. 1 is estimated using theoretical radiation, possibly overestimated given the lack of information about cloud cover. A preliminary assessment of such effect using precipitation events/intensity as a proxy for cloud cover was pursued, but no acceptable results were obtained (compare with, e.g., Soncini et al. 2016). Initial ice thickness assessment using back-calculation

from Eq. 3 may have further introduced a *bias* in ice thickness/velocity assessment. The available weather data are for sites somewhat far from the glaciers, and no near glacial stations are present at now. Coupling remote-sensing investigations with observation during our field surveys in 2014, we were able to map total (i.e., including debris cover) ice-covered areas, estimated into 7.28 ± 0.03 km^2, including 1.82 ± 0.01 km^2 of debris-covered area. Comparing our measurements with those reported by previous authors, mapped solely on the basis of satellite imagery (Sarikaya 2012; Yavaşli et al. 2015), we note that they had underestimated the true extent of glacial coverage of the volcano. Their estimation of ca. 5.66 ± 0.57 km^2 (in 2011) possibly suffered from the incomplete detection of debris-covered ice sectors, and in this sense, our work improves the knowledge of the ongoing processes on the Ararat glaciers. This in turn allowed a more proper implementation of the ice flow/melt model, by accounting for ice fluxes under debris cover at the lowest altitudes. We do not know about previous attempts at modeling the ice flow of the Ararat glaciers, and we cannot benchmark our results accordingly. However, the Poly-Ice model seemingly displayed acceptable results in our preliminary attempt at modeling the dynamics of this complex glacier apparatus, and indeed represents a valuable tool to highlight the processes underpinning glacier retreat here, and possibly to figure out future evolutions under climate change.

6 Conclusions

We demonstrated how recent downwasting of glaciers on the Ararat mountain is actually occurring, as documented in the previous literature, and we even put forward some conjectures about the main causes of such phenomena. Clearly during the four last decades, significantly increasing temperature affected shrinking of the ice bodies. Substantially constant precipitation could not make up by accumulation at the highest altitudes. The use of our deterministic, physically based Poly-Ice model, able to represent the response of the case study glaciers to climatic variations, provides further ground to our conjectures. Ever since the 1990s under ever-increasing temperatures, the ice bodies responded rapidly to yearly fluctuation of temperature. Poly-Ice depicts how winter snow accumulation at the highest altitudes largely decreased ever since the 1980s (when a maximum was seen), and in spite of a slight recover during the last decade, such lack of snow resulted into ice loss under increasing temperature. Potential future improvements may include use of actual radiation data (whenever they would become available) and use of multiple snow cover images for validation of the modeled snow area. Notice however that given the small extent of the simulation area, and the 30-m resolution of the model, fine resolution snow cover images would probably be necessary for the purpose, so the normally adopted medium-resolution satellites (e.g., MODIS, Bocchiola et al. 2011) may not be very helpful here, and other sources may be used, with more complex and demanding procedure (e.g., Landsat TM, Soncini et al. 2017). We did not possess observed data of ice melt, on either bare or debris-covered ice, as we gathered on the field in other areas (e.g., Bocchiola et al. 2010; Minora et al. 2015a, b; Soncini et al. 2016, 2017). However, topographic and climate conditions on the Ararat ice cap make direct ice melt investigation according to standard glaciological methods quite complex. Accordingly, we relied upon the hypothesis of constant (i.e., valid on average) melt factors, which is a weak one especially on debris cover, given complex energy budget therein (e.g., Bocchiola et al. 2015), and we used indirect calibration against ICA images. New expeditions may be targeted at tackling such issue, and provide field assessment of ice melting.

Further effort may be placed into projection of future climate in the area, for assessment of potential glaciers evolutions, e.g., under climate scenarios from IPCC (e.g., Soncini et al. 2015, 2016; Bocchiola et al. 2018). The authors here gathered recently noteworthy experience in such exercise, which however entails large uncertainty depending upon the adopted models and representative concentration pathways (RCPs) (from RCP2.6, with the least temperature increase, to RCP8.5 with the greatest increase).

Our results confirm the ongoing mass loss of the glaciers of the iconic Ararat mountain, paradigmatic of the continental glacial retreating phase in Europe and Asia, provide mechanistic explanation of such retreat, and even deliver a numerical, physically based tool to mimic future evolution of this topographically complex glaciers under future climate scenarios. Eventually, our findings deliver a hopefully interesting contribution to the recent global scientific debate about climate change and subsequent impacts on ice bodies, landscapes, and water resources.

Acknowledgments The results here presented partly rely on findings from the 2014 ARARAT Expedition, organized by the Central Scientific Committee of the Italian Alpine Club (CSC-CAI). Researchers from the University of Milano, University of Milano-Bicocca, Politecnico di Milano, University of Florence, University of Pisa, personnel from the Environmental Protection Agency (ARPA-Lombardia, Centro Nivometeorologico Bormio), and from the Medical Commission of the Italian Alpine Club who were part to the expedition. RSA and DB took part in the expedition. The authors are grateful to all the people who participated in the field campaign, namely Carlo Alberto Garzonio, Andrea Franzetti, Riccardo Avanzinelli, Simone Tommasini, Raffaello Cioni, Eraldo Meraldi, Andrea Franzetti, Giulia Enrione, and Luigi Vanoni for medical support and the local guide Burhan Cevarun for help with field activities. The Pleiades and SPOT data were provided by the European Space Agency (ESA project: Geomorphological mapping and recent glacier evolution of the Mount Ararat volcanic complex through SPOT and PLEIADES images ID-32011).

References

Abich G (1847) Geognostische Reise zum Ararat der und Verschuttung des Thales von Arguri im Jahre 1840. [Geological news of a journey to Ararat and particularly the collapse of the valley of Arguri in 1840]. Monatsber Verh Ges Erdkd Berlin, Neue Folge 4:28–62

Aili T, Soncini A, Bianchi A, Diolaiuti G, Bocchiola D (2018) A method to study hydrology of high altitude catchments: the case study of the Mallero river, Italian Alps. Theoret Appl Climatol:1–22. https://doi.org/10.1007/s00704-017-2366-4

Akçar N, Yavuz V, Yesilyurt S, Ivy-Ochs S, Reber R, Bayrakdar C, Schluchter C (2015) Synchronous last glacial maximum across the Anatolian peninsula, 2015. Geological Society, Special Publications. https://doi.org/10.1144/SP433.7

Allen RG, Trezza R, Tasumi M (2006) Analytical integrated functions for daily solar radiation on slopes. Agric For Meteorol 139(1–2):55–73

Azzoni RS, Senese A, Zerboni A, Maugeri M, Smiraglia, Diolaiuti GA (2016) Estimating ice albedo from fine debris cover quantified by a semi-automatic method: the case study of Forni glacier, Italian alps. Cryosphere 10:665–679

Azzoni RS, Zerboni A, Pelfini M, Diolaiuti GA (2017) Geomorphology of Mount Ararat/Ağri Dağı (Ağri Dağı Milli Parki, Eastern Anatolia, Turkey). Journal of Maps 13(2):182–190

Baumann S, Winkler S (2010) Parameterization of glacier inventory data from Jotunheimen/Norway in comparison to the European Alps and the Southern Alps of New Zealand. Erdkunde 64:2,155–2,177

Berlitz C (1987) The lost ship of Noah. Putnam Press, New York 167 pp

Blumenthal MM (1958) From Mount Ağrı to Kaçkar Mountains. Die Alpen 34:125–137

Bocchiola D (2010) Regional estimation of snow water equivalent using kriging: a preliminary study within the Italian Alps. Physical Geography and Quaternary Dynamics GFDQ 33:3–14

Bocchiola D (2014) Long term (1921-2011) changes of Alpine catchments regime in Northern Italy. Adv Water Resour 70:51–64

Bocchiola D, Diolaiuti G (2010) Evidence of climate change within the Adamello glacier of Italy. Theor Appl Climatol 100(3–4):351–369

Bocchiola D, Diolaiuti G (2013) Recent (1980-2009) evidence of climate change in the upper Karakoram, Pakistan. Theor Appl Climatol 113(3–4):611–641

Bocchiola D, Groppelli B (2010) Spatial estimation of Snow Water Equivalent at different dates within the Adamello Park of Italy. Cold Regions Science and Technology 63(3):97-109

Bocchiola D, Rosso R (2007) The distribution of daily snow water equivalent in the Central Italian Alps. Adv Water Resour 30:135–147

Bocchiola D, Bianchi Janetti E, Gorni E, Marty C, Sovilla B (2008) Regional evaluation of three day snow depth frequency curves for Switzerland. NHESS 8:685–705

Bocchiola D, Mihalcea C, Diolaiuti G, Mosconi B, Smiraglia C, Rosso R (2010) Flow prediction in high altitude ungauged catchments: a case study in the Italian Alps (Pantano Basin, Adamello Group). Adv Water Resour 33:1224–1234

Bocchiola D, Diolaiuti GA, Soncini A, Mihalcea C, D'Agata C, Mayer C, Lambrecht A, Rosso R, Smiraglia C (2011) Prediction of future hydrological regimes in poorly gauged high altitude basins: the case study of the upper Indus, Pakistan. Hydrol Earth Syst Sci 15:2059–2075

Bocchiola D, Senese A, Mihalcea C, Mosconi B, D'Agata C, Smiraglia C, Diolaiuti G (2015) An ablation model for debris covered ice: the case study of Venerocolo glacier (Italian Alps). Physical Geography and Quaternary Dynamics GFDQ 38(2):13–128

Bocchiola D, Soncini A, Senese A, Diolaiuti G (2018) Modelling hydrological components of the Rio Maipo of Chile, and their prospective evolution under climate change. Climate 6(3):1–27

Brohan P, Kennedy JJ, Harris I, Tett SFB, Jones PD (2006) Uncertainty estimates in regional and global observed temperature changes: a new dataset from 1850. J Geophys Res 111:D12106

Çiner A (2004) Turkish glaciers and glacial deposits. In: Ehlers J, Gibbard PL (eds) Quaternary glaciations-extent and chronology. Part I: Europe. Elsevier, Amsterdam, pp 419–129

Confortola G, Soncini A, Bocchiola D, (2013) Climate change will affect water resources in the Alps: a case study in Italy, Journal of Alpine Research. RGA/JAR 101(3)

Cuffey KM, Paterson WSB (2010) The physics of glaciers, 4th Edition. Academic Press, Amsterdam, pp 704

De Silva S, Lindsay JM (2015) Chapter 15—primary volcanic landforms. In: Sigurdsson H (ed) The encyclopedia of volcanoes, 2nd edn. Academic, Amsterdam, pp 273–297

Diolaiuti G, D'Agata C, Meazza A, Zanutta A, Smiraglia C (2009) Recent (1975-2003) changes in the Miage debris-covered glacier tongue (Mont Blanc, Italy) from analysis of aerial photos and maps. Geogr Fis Din Quat 32:117–127

Diolaiuti G, Bocchiola D, D'Agata C, Smiraglia C (2012a) Evidence of climate change impact upon glaciers' recession within the Italian Alps: the case of Lombardy glaciers. Theor Appl Climatol 109(3–4):429–445

Diolaiuti G, Bocchiola D, Vagliasindi M, D'Agata C, Smiraglia C (2012b) The 1975-2005 glacier changes in Aosta Valley (Italy) and the relations with climate evolution. Prog Phys Geogr 36(6):764–785

Garzonio CA (2015) La ricerca scientifica sul monte Ararat: La spedizione del Comitato scientifico centrale del CAI sul grande vulcano anatolico. [The scientific research on mounta Ararat: the CAI scientific committee expedition on the big Anatolian volcano] Montagna 360°. Marzo 2015:38–43

Groppelli B, Soncini A, Bocchiola D, Rosso R, (2011) Evaluation of future hydrological cycle under climate change scenarios in a mesoscale Alpine watershed of Italy. NHESS 11:1769-1785

Hughes PD (2014) Little ice age glaciers in the Mediterranean mountains. Méditerranée 122:63–79

Imhof E (1956) The Ararat. Die Alpen 32:1–14

Karakhanian AS, Djrbashian R, Trifonov VG, Philip H, Arakelian S, Avagian A (2002) Holocene-historical volcanism and active faults as natural risk factors for Armenia and adjacent countries. J Volcanol Geotherm Res 113:319–344

Keskin M (2003) Magma generation by slab steepening and breakoff beneath a subduction-accretion complex: an alternative model for collision-related volcanism in Eastern Anatolia, Turkey. Geophys Res Lett 30:8046

Kirkbride M (2011) Debris-covered glaciers. In: Singh VP, Singh P, Haritashya UK (eds) Encyclopedia of snow, ice and glaciers. Springer, Dordrecht, pp 190–192

Kumar L, Skidmore AK, Knowles E (1997) Modelling topographic variation in solar radiation in a GIS environment. Int J Geogr Inf Sci 11(5):475–497

Kurter A (1991) Glaciers of Middle East and Africa-glaciers of Turkey. In RS Williams & JG Ferrigno (eds) Satellite image Atlas of the World. USGS Professional Paper, pp 1386–G1

Migliavacca G, Confortola A, Soncini A, Diolaiuti G, Smiraglia C, Barcaza G, Bocchiola D (2015) Hydrology and potential climate changes in the Rio Maipo (Chile). Physical Geography and Quaternary Dynamics GFDQ 38(2):155–168

Minora U, Senese A, Bocchiola D, Soncini A, D'agata C, Ambrosini R, Mayer C, Lambrecht A, Vuillermoz E, Smiraglia C, Diolaiuti G (2015a) A simple model to evaluate ice melt over the ablation area of glaciers in the Central Karakoram National Park, Pakistan. Ann Glaciol 56(70):202–216

Minora U, Godone D, Lorenzini S, D'Agata C, Bocchiola D, Barcaza GS, Smiraglia C, Diolaiut GA (2015b) 2008-2011 snow cover area (SCA) variability over 18 watersheds of the Central Chile through

MODIS data. Physical Geography and Quaternary Dynamics, GFDQ 38(2):169–174

Minora U, Bocchiola D, D'Agata C, Maragno D, Mayer C, Lambrecht A, Diolaiuti GA (2016) Glacier area stability in the Central Karakoram National Park (Pakistan) in 2001–2010: the "Karakoram Anomaly" in the spotlight. Prog Phys Geogr 40:629–660. https://doi.org/10.1177/0309133316643926

Narama C, Kääb A, Murataly D, Abdrakhmatov K (2010) Spatial variability of recent glacier area changes in the Tien Shan Mountains, Central Asia, using Corona (~1970), Landsat (~2000), and ALOS (~2007) satellite data. Glob Planet Chang 71(1–2):42–54

Notsu K, Fujitani T, Ui T, Matsuda J, Ercan T (1995) Geochemical features of collision-related volcanic rocks in central and eastern Anatolia, Turkey. Turkey Research 64:171–191

Oerlemans J (2001). Glaciers and climate change. A. A. Balkema Publishers, Brookfield, pp 148

Ohlendorf C, Niessenn F, Weissert H (1997) Glacial varve thickness and 127 years of instrumental climate data: a comparison. Clim Chang 36:391–411

Osborn TJ (2004) Simulating the Winter North Atlantic Oscillation: the roles of internal variability and greenhouse gas forcing. Clim Dyn 22:605–623

Parrot F (1859) Journey to Ararat. Harper and Brothers, NewYork 389 pp

Salerno F, Thakuri S, Smiraglia C, D'Agata C (2014) Tracing glacier changes since the 1960s on the south slope of Mt. Everest (central southern Himalaya) using optical satellite imagery. Cryosphere 8:1297–1315

Sarikaya MA (2012) Recession of the ice cap on mount Ağrı (Ararat), Turkey, from 1976 to 2011 and its climatic significance. J Asian Earth Sci 46:190–194

Sarikaya MA, Çiner A (2014) Late quaternary glaciations in the eastern Mediterranean. In: Hughes PD, Woodward JC (eds) Quaternary glaciation in the Mediterranean mountains. Elsevier, Amsterdam, p 433

Sarikaya MA, Tekeli AE (2014) Satellite inventory of glaciers in Turkey. In: Kargel JS, Leonard GJ, Bishop MP, Kääbm A, Raup BH (eds) Global land ice measurements from space. Springer, Berlin, pp 465–480

Sarikaya MA, Çiner A, Zreda M (2011) Quaternary glaciations of Turkey. In: Ehlers J, Gibbard PL, Hughes PD (eds) Developments in quaternary science, vol 15. Elsevier, Amsterdam, pp 393–403

Seiz G, Foppa N (2007) National climate observing system (GCOS Switzerland). Publication of the Federal Office of Meteorology and Climatology MeteoSwiss and ProClim, Geneva 92 pp

Senese A, Maugeri M, Ferrari S, Confortola G, Soncini A, Bocchiola D, Diolaiuti G (2016) Modelling shortwave and longwave downward radiation and air temperature driving ablation at the Forni glacier (Stelvio National Park, Italy). Geogr Fis Din Quat 39(1):89–100

Simkin T, Siebert L (1994) Volcanoes of the world, 2nd edn. Geoscience Press in Association with the Smithsonian Institution Global Volcanism Program, Tucson

Smiraglia C, Diolaiuti GA (2011) Epiglacial morphologies. In: Singh VP, Singh P, Haritash UK (eds) Encyclopedia of snow, ice and glaciers. Springer, Dordrecht, pp 262–268

Smiraglia C, Azzoni RS, D'Agata C, Maragno D, Fugazza D, Diolaiuti GA (2015) The evolution of the Italian glaciers from the previous data base to the New Italian inventory. Preliminary considerations and results. Geogr Fis Din Quat 38(1):79–87

Soncini A, Bocchiola D, Confortola G, Bianchi A, Rosso R, Mayer C, Lambrecht A, Palazzi E, Smiraglia C, Diolaiuti G (2015) Future hydrological regimes in the upper Indus basin: a case study from a high altitude glacierized catchment. J Hydrometeorol 16(1):306–326

Soncini A, Bocchiola D, Confortola G, Minora U, Vuillermoz E, Salerno F, Viviano G, Shrestha D, Senese A, Smiraglia C, Diolaiuti G (2016) Future hydrological regimes and glacier cover in the Everest region: the case study of the Dudh Koshi basin. Sci Total Environ 565:1084–1101

Soncini A, Bocchiola D, Azzoni RS, Diolaiuti G (2017) A methodology for monitoring and modeling of high altitude Alpine catchments. Prog Phys Geogr 41(4):393–420

Stokes CR, Gurney SD, Shahgedanova M, Popovnin V (2006) Late-20th-century changes in glacier extent in the Caucasus Mountains, Russia/Georgia. J Glaciol 52(176):99–109

Stokes CR, Popovnin V, Aleynikov A, Gurney SD, Shahgedanova M (2007) Recent glacier retreat in the Caucasus Mountains, Russia, and associated increase in supraglacial debris cover and supra−/proglacial lake development. Ann Glaciol 46:195–203

Vögtle T, Schilling K (1999) Digitizing maps. In: Bähr HP, Vögtle T (eds) GIS for environmental monitoring. Schweizerbart, Stuttgart, pp 201–216

Wallinga J, van de Wal RSW (1998) Sensitivity of Rhonegletscher, Switzerland, to climate change: experiments with a one-dimensional flow line model. Journal of Glaciology 44(147): 383-393

Williams RS, Ferrigno JG (1991) Glaciers of the Middle East and Africa. In: RS Williams & JG Ferrigno (eds) Satellite image atlas of the world. USGS professional paper 1386–G

Wüthrich C, Begert M, Scherrer SC, Croci-Maspoli M, Appenzeller C, Weingartner R (2008) Analyses of newly digitised snow series over the last 100 years+in Switzerland. In: Abstract Volume 6, abstract no. 6.29, 6th Swiss Geoscience Meeting Lugano, 21–23, November 2008

Yavaşli DD, Tucker CJ, Melocik KA (2015) Change in the glacier extent in Turkey during the Landsat era. Remote Sens Environ 163:32–41

Yilmaz Y, Güner Y, Saroğlu F (1998) Geology of the quaternary volcanic centres of the East Anatolia. J Volcanol Geotherm Res 85:173–210

Yue S, Wang CY (2002) Applicability of pre-whitening to eliminate the influence of serial correlation on the Mann-Kendall test. Water Resour Res 38(6):1068

Zhang X, Vincent LA, Hogg WD, Niitsoo A (2000) Temperature and precipitation trends in Canada during the 20th century. Atmosphere-Ocean 38(3):395–429